

A linear near-IR Tully-Fisher relation for giant and dwarf late-type galaxies

D. Pierini and R.J. Tuffs

Max-Planck-Institut für Kernphysik, Saupfercheckweg 1, D-69117 Heidelberg, Germany

Received 13 August 1998 / Accepted 15 December 1998

Abstract. We present the near-IR (K' -band, i.e.: $\lambda = 2.1 \mu\text{m}$) Tully-Fisher (TF) relation for a sample of 50 giant and dwarf late-type galaxies, selected from the Virgo Cluster Catalogue. We find that $L \propto V_{Max}^4$ along a range of 8 K' -mag for galaxies with different Hubble types (from Sa to Im-BCD), phenomenologies, structures, star-formation histories, masses, dark-to-luminous mass ratios, metallicities and, perhaps, ages. The linearity of the near-IR TF relation is in contrast with recent determinations of the optical TF relations for samples of extreme late-type and dwarf galaxies. The near-IR TF law is in agreement both with the expectation from the Fundamental Plane for disk systems and with the scenario of self-regulating star-formation in disks. The previous results suggest that the TF relation reflects the connection between the structural/dynamical properties and the star-formation process of both giant and dwarf late-type galaxies, through a gas supply for star-formation regulated by the gravitational potential of the galaxy.

Key words: galaxies: distances and redshifts – galaxies: fundamental parameters – galaxies: irregular – galaxies: structure – infrared: galaxies

1. Introduction

The existence of a relation between the maximum rotational velocity and the luminosity of giant high surface brightness (HSB) late-type galaxies has long been known (Tully & Fisher 1977). Aaronson et al. (1979) gave an “a posteriori” justification of the near-IR (NIR) Tully-Fisher law ($L \propto V_{Max}^4$), based on the virial theorem and on the three following assumptions: 1) “all galaxies have the same mass profiles and rotation curves as a function of some dimensionless scale-length”; 2) “all galaxies have the same central mass surface density”; 3) “all galaxies have the same mean mass-to-light ratio (M/L)”.

Recent observational results have disclaimed the second assumption (de Jong 1996; Giovanelli et al. 1997). Moreover, Zwaan et al. (1995) have shown that the low surface brightness (LSB) late-type galaxies follow the same B-band TF relation as the HSB ones, even though their mass-to-light ratios are

very different (McGaugh & Bothun 1994; De Blok & McGaugh 1997). Some of the previous seminal ideas have been restated by Burstein et al. (1997), who claimed that the TF relation is a projection of the so-called “ κ -space” three dimensional parameter system (mass, mass-to-light ratio and surface brightness) of late-type galaxies. From a theoretical point of view, models explaining the TF law belong to two broad distinct categories: one that derives the TF relation as a consequence of the self-regulating star-formation in disk galaxies (e.g., Silk 1997); the other which sees the TF relation as a direct consequence of the equivalence between mass and rotational velocity of disks (e.g., Mo et al. 1998).

As a matter of fact, none of the current available models of galaxy formation, independent of whether or not related to specific cosmological scenarios, is definitive in explaining the Tully-Fisher relation (Eisenstein & Loeb 1996; Dalcanton et al. 1997; Mo et al. 1998; Steinmetz & Navarro 1998; Elizondo et al. 1998; but see Somerville & Primack 1998). This is also because of the lack of observational constraints. In particular, dwarf galaxies have been mostly ignored till nowadays, even in one of the most complete studies of the TF relation for nearby galaxies (Giovanelli et al. 1997). Recent results from optical surveys of extreme late-type and dwarf galaxies (Matthews et al. 1998; Stil & Israel 1998) have found an increasing deviation from the TF relation with decreasing luminosity. There is no “a priori” expectation that dwarf late-type galaxies follow the same TF relation of giant spiral and irregular galaxies, since the mass-to-light ratio, dynamics, structure, metallicity and age are found/supposed to be very different. However, van Zee et al. (1998) have recently demonstrated that BCD galaxies are rotationally supported systems.

The Virgo Cluster provides a sufficiently well known sample of both dwarf and giant galaxies, because of its proximity to us, and the Virgo Cluster Catalogue (VCC) of Binggeli et al. (1985, 1993) gives reliable cluster memberships, limiting the effect of the Malmquist bias. Previous works on the Tully-Fisher relation based on the Virgo late-type galaxies and also on the near-IR bands (where magnitudes are less affected by internal extinction and by gradients in the ages of the stellar populations). However, they do not sample a wide range of luminosities (Peletier & Willner 1991; Gavazzi et al. 1998) and/or Hubble types (also extended to dwarf galaxies) while at the same time using a large

data set of camera magnitudes (Aaronson et al. 1979; Pierce & Tully 1988; Kraan-Korteweg et al. 1988). For all these reasons, the complete sample of VCC giant and dwarf galaxies, imaged by Boselli et al. (1997) in the K' -band, is a powerful tool for a new study of the NIR Tully-Fisher relation, aimed at investigating the connection between scaling relations and star-formation properties of disk galaxies of different mass from the observational point of view (cf. Silk 1997; Elizondo et al. 1998).

The outline of the paper is as follows: Sect. 2 presents the sample; Sect. 3 describes the procedure adopted for the determination of the TF relation, while Sect. 4 discusses its robustness. We discuss the present results in terms of the connection between dynamical equilibrium and self-regulating star-formation in Sect. 5. Sect. 6 reports on our conclusions.

Hereafter we adopt $H_0 = 100 \text{ km s}^{-1} \text{ Mpc}^{-1}$ and a distance of 11 Mpc for Virgo.

2. The sample

The present sample is selected from the VCC (Binggeli et al. 1985), which is complete to $B_T \leq 18$ mag, according to the following criteria:

- 1) $B_T \leq 16$ mag;
- 2) Hubble type later than S0a;
- 3) cluster membership according to Binggeli et al. (1993);
- 4) sky distribution according to Boselli et al. (1997);
- 5) $35^\circ < i < 80^\circ$;
- 6) no interacting system (see Tutui & Sofue 1997);
- 7) $\sigma_W/W < 1/3$, where W is the HI linewidth (full width at 20% level of I/I_{max}) in km s^{-1} and σ_W its error.

K' -band ($\lambda = 2.1 \mu\text{m}$) magnitudes were derived by synthetic aperture photometry, integrating counts along concentric circular annuli around the galaxy center to provide growth curves up to the isophotal diameter D_{25} (corresponding to the 25th B-mag arcsec⁻² isophote), and were corrected for Galactic and internal extinction (as in the K -band, i.e.: $\lambda = 2.2 \mu\text{m}$), according to Gavazzi & Boselli (1996). The overall photometric accuracy is ~ 0.1 mag.

HI linewidths have been taken in a consistent way from Bottinelli et al. (1990), Hoffman et al. (1987) and Huchtmeier & Richter (1989). Corrections for turbulent/ z -motions come from Huchtmeier & Richter (1989), for both giant and dwarf galaxies, even though for the latter a well-founded correction recipe is still lacking. Velocities were deprojected adopting the constant value of 0.2 for the intrinsic flattening (see Yasuda et al. 1997).

Among the 84 galaxies of the Virgo-ISO sample, later than S0a, observed by Boselli et al. (1997), only 69 have HI line measurements in the literature. Eight of the 15 galaxies without linewidths are Sa, two Sm and five Im-BCD. Only 2/15 objects are rejected according to criteria 5 and 6. Thirteen of the 69 objects do not satisfy our inclination criteria. Moreover, there are 4 interacting galaxies (VCC 1043, 1673, 1676, 1972) and 2 galaxies with low quality linewidths. The resultant sample consists of 50 objects (24 with $1 \leq T \leq 8$ and 26 with $9 \leq T \leq 11$, where T is the RC3 type - de Vaucouleurs et al. 1991) and its completeness is at least 79%.

We remark that no selection criterion has been adopted on the basis of HI-deficiency (Haynes & Giovanelli 1984) of the galaxies. However, for the HI-deficient galaxies of the present sample mapped in HI by Cayatte et al. (1990) and with extended optical rotation curves available in the literature (VCC 836, 873, 1110, 1690, 1727), we did not find any systematic difference between the two sets of velocities. Moreover, for the latter galaxies, Schoeniger & Sofue (1997) show that CO and HI linewidths are in agreement.

The optical, NIR and dynamical properties of the resultant sample of 50 galaxies are given in Table 1, as follows:

- Col.1: VCC denomination;
- Col.2,3: celestial coordinates (epoch=1950.0);
- Col.4: morphological classification (VCC);
- Col.5,6: major axis ($a_{25.5}$, measured at the 25.5 B-mag arcsec⁻² isophote) and ratio between major and minor axes;
- Col.7: B_T (VCC);
- Col.8: K' apparent magnitude;
- Col.9: HI observed linewidth (W) and its error (σ_W).

3. The near-infrared TF relation

The high reliability of the cluster membership for the VCC galaxies (Binggeli et al. 1993) gives us the opportunity of using the face-on apparent magnitudes, instead of the absolute ones, in the present determination of the Tully-Fisher relation (cf. Sandage et al. 1995). However, the cluster depth effect is discussed in the validation of our results (Sect. 4).

The equation of the Tully-Fisher relation is obtained through two different algorithms, without data rejection. The first one is based on the minimization of the quadratic sum of the perpendicular distances between the data points and the best-fit line, following the method explained in Condon et al. (1991). Therefore, both the “direct” and “inverse” relations are derived in order to obtain the “true” TF relation. As a consequence, the uncertainties in the observational and the adopted corrections, both for the magnitudes and the velocities, are taken into account in the determination of the true TF relation, but separately! The inclinations are derived assuming a constant intrinsic axial ratio of 0.2, and a standard uncertainty of $\pm 5^\circ$ is adopted.

Without applying corrections for turbulent/ z -motions, the equation of the true TF relation is:

$$K'_0 = -10.08(\pm 0.10) \times \log(V_{Max}) + 30.66(\pm 0.20) \quad (1a)$$

($R^2 = 0.94$); in the opposite case the fit is:

$$K'_0 = -10.72(\pm 0.23) \times \log(V_{Max}) + 31.40(\pm 0.43) \quad (1b)$$

($R^2 = 0.94$), where K'_0 and V_{Max} are, respectively, the face-on apparent magnitude and the inclination corrected maximum velocity.

The second algorithm executes a bivariate least-squares fit, taking into account the uncertainties in both the x - and y -variables at the same time. It is implemented in the task “FITEXY” of the Numerical Recipes. In correspondence with the two previous cases, we obtain:

$$K'_0 = -9.82(\pm 0.13) \times \log(V_{Max}) + 30.06(\pm 0.25) \quad (2a)$$

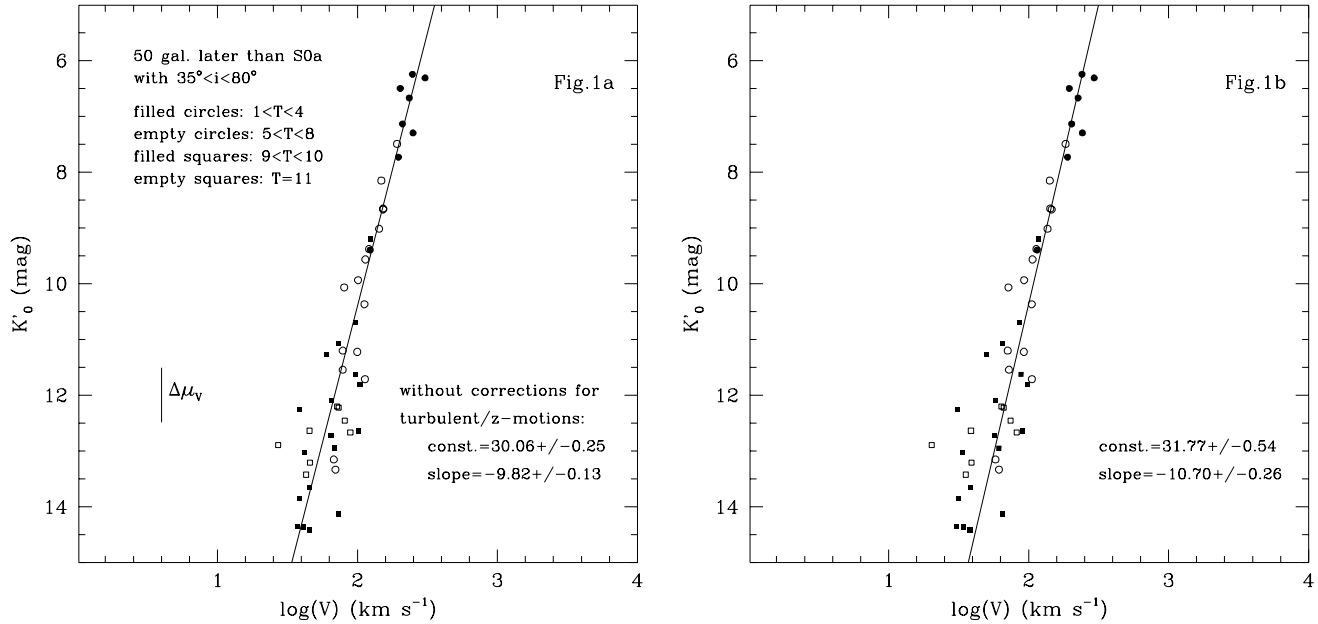


Fig. 1a and b. The K' -band Tully-Fisher relation for the galaxies of the present sample. Hereafter, different symbols denote galaxies of different Hubble types (see panel a). The straight line represents the fit obtained with **b** and without **a** applying corrections for turbulent/z-motions (Eqs. 2). In panel a we also plot the shift in magnitude caused by the size of Virgo.

($R^2 = 0.94$) (see Fig. 1a) and:

$$K'_0 = -10.70(\pm 0.26) \times \log(V_{Max}) + 31.77(\pm 0.54) \quad (2b)$$

($R^2 = 0.94$) (see Fig. 1b). We note that both sets of Eqs. 1 and 2 are consistent within the errors. However, hereafter we use Eqs. 2a,b, since the algorithm used for their determination is more robust. Table 2 shows the statistical moments of the distributions of the residuals of the fits of Eqs. 2a,b.

In Fig. 1a we also plot the characteristic shift in magnitude that may be caused by the depth of Virgo, taken as the difference in distance modulus between cluster A ($\mu_0 = 30.78 \pm 0.07$), associated with M87, and cluster B ($\mu_0 = 31.76 \pm 0.09$), offset to the south (from Gavazzi et al. 1998) and associated with M49. However, we note that galaxies within 1.5 degrees from M49 are not included in the sample (cf. Boselli et al. 1997). The dispersion of the present sample of galaxies in Figs. 1a,b is mainly within 0.98 mag along the whole range of the inclination corrected maximum velocity.

Caution is necessary to interpret the result because of the presence of the slow rotators, whose observational errors and corrections for turbulent/z-motions are comparable and relevant with respect to their observed HI linewidths. However, we note that the value of the TF slope is marginally consistent with an $L \propto V_{Max}^4$ law, when this correction is applied.

In order to avoid extra model dependences on the present results and to compare them with those ones in the literature, hereafter we consider the formulation of the TF relation obtained without any corrections for turbulent/z-motions (cf. Yasuda et al. 1997) of Eq. 2a. Moreover, we stress that previous authors (e.g. Pierce & Tully 1988; Peletier & Willner 1993) determined mainly the direct TF relation, relying on the small percentual errors of the velocities of the fastest (within the range 2.2–2.8 in

log(W)) of their (consequently) bright sampled galaxies. When the grasp in the luminosity function of the late-type galaxies is extended to fainter magnitudes, the uncertainties on the observed velocities highly bias the slope of the direct TF relation. This effect is shown by the comparison of the slope of the direct TF relation (-8.67 ± 0.06) and the inverse of the slope of the inverse TF relation (-10.10 ± 0.10) obtained through the algorithm of Condon et al. (1991). With the previous caveats in mind, we claim that the present slope of -9.82 ± 0.13 is consistent with the previous derivations of the NIR TF relation, i.e.: Aaronson et al. (1979) (-9.67 ± 0.24), Kraan-Korteweg et al. (1988) (-9.81), Pierce & Tully (1988) (-9.25 ± 0.43), Peletier & Willner (1993) (-10.2 ± 0.6). We note that Kraan-Korteweg et al. extrapolated a linear relation B-H vs. W to the low velocity region in order to derive the H-band magnitudes of the galaxies at the faint end of their sample.

Therefore, the present analysis confirms and strengthens previous claims that the NIR Tully-Fisher relation is linear, over a range of 8 magnitudes and over the whole range of optical morphologies (from Sa to Im-BCD). As a consequence, we conclude that even BCD galaxies are rotationally supported systems, in agreement with van Zee et al. (1998).

4. The cluster incompleteness bias and other potential biases of the present sample

The present sample has been selected in the optical and suffers incompleteness due to the combination of low statistics, selection criteria (cf. Sect. 2) and the cluster depth effect. Here we discuss the effects of such incompleteness on the previous results.

Table 1. Galaxy parameters

Denomination VCC	R.A. (1950) hh mm	DEC (1950) dd mm	Hubble Type	$a_{25.5}$ '	$a_{25.5}/b_{25.5}$	B_T mag	K' mag	V_{Max} kms^{-1}
17	12 07.48	14 38.4	Im	1.4	2.0	15.2	14.0	69 ± 20
24	12 08.05	12 02.3	BCD	0.8	2.7	14.9	12.8	86 ± 20
66	12 10.23	11 08.8	SBc	6.6	2.8	11.9	8.8	286 ± 6
87	12 11.13	15 43.9	Sm	1.8	2.0	15.0	13.1	121 ± 20
92	12 11.26	15 10.8	Sb:	12.0	3.7	10.9	6.5	476 ± 4
152	12 12.97	09 51.8	Scd	2.3	2.2	13.5	9.5	206 ± 8
159	12 13.14	08 33.8	Im	0.9	2.0	15.1	14.6	80 ± 20
318	12 16.50	09 08.1	SBcd	2.1	1.7	14.0	11.8	187 ± 10
459	12 18.66	17 54.9	BCD	0.6	2.3	14.9	12.6	150 ± 20
460	12 18.69	18 39.7	Sa pec	6.3	1.7	11.2	7.3	381 ± 9
692	12 21.49	12 28.9	Sc	3.6	1.5	13.0	10.1	116 ± 6
836	12 23.23	12 56.3	Sab	6.3	4.1	11.8	8.0	385 ± 5
873	12 23.58	13 23.4	Sc	4.9	3.4	12.6	8.4	286 ± 6
912	12 24.00	12 53.3	SBbc	3.6	1.7	13.0	9.5	186 ± 5
950	12 24.36	11 50.3	Sm	2.1	2.0	14.5	13.8	81 ± 3
995	12 24.82	11 08.6	Sc	2.5	9.9	15.3	12.0	160 ± 15
1110	12 25.97	17 21.7	Sab pec	7.6	1.5	10.9	6.7	330 ± 9
1189	12 26.93	07 02.9	Sc	2.0	1.7	13.7	11.3	130 ± 10
1356	12 28.86	11 46.0	Sm/BCD	0.9	2.5	14.9	12.8	167 ± 10
1379	12 29.14	17 07.8	SBc	3.5	1.9	12.6	9.7	196 ± 6
1410	12 29.54	16 57.8	Sm	1.3	1.9	14.6	11.9	181 ± 8
1448	12 30.13	13 03.0	Im or dE	2.9	1.3	13.9	11.3	74 ± 16
1486	12 30.65	11 37.2	S pec	0.9	1.4	15.3	11.7	140 ± 13
1554	12 31.78	06 44.7	Sm	3.2	2.6	12.3	9.4	229 ± 5
1569	12 32.00	13 46.9	Scd:	1.3	1.5	15.0	13.4	107 ± 15
1575	12 32.11	07 26.2	SBm pec	1.3	1.4	14.0	10.7	127 ± 9
1581	12 32.20	06 34.7	Sm	1.3	1.3	14.5	12.7	125 ± 20
1675	12 34.04	08 19.8	pec	1.0	1.7	14.5	12.4	64 ± 20
1686	12 34.21	13 32.0	Sm	3.5	1.6	13.9	11.2	118 ± 20
1690	12 34.31	13 26.4	Sab	13.2	2.0	10.2	6.6	360 ± 13
1699	12 34.50	07 12.3	SBm	1.4	1.9	14.1	12.2	112 ± 10
1725	12 35.15	08 50.0	Sm/BCD	1.4	1.6	14.5	12.3	114 ± 20
1726	12 35.20	07 22.7	Sdm	1.6	1.3	14.5	13.2	87 ± 20
1727	12 35.20	12 05.6	Sab	7.8	1.3	10.6	6.4	362 ± 9
1730	12 35.27	05 38.6	Sc/Sa	2.7	1.3	12.6	8.7	196 ± 13
1789	12 36.81	05 12.8	Im	0.9	1.8	15.1	12.8	109 ± 20
1791	12 36.88	08 14.2	SBm/BCD	1.6	2.0	14.7	12.4	130 ± 13
1804	12 37.14	09 40.4	Im/BCD	1.3	2.5	15.5	13.4	86 ± 13
1811	12 37.35	15 34.4	Sc	2.7	1.5	12.9	10.0	152 ± 12
1918	12 39.76	06 00.8	Im	0.8	2.8	15.8	14.6	78 ± 13
1929	12 40.11	14 37.8	Scd	3.1	2.3	13.8	10.5	206 ± 10
1932	12 40.17	14 34.2	Sc	3.6	3.3	13.2	9.3	280 ± 13
1952	12 40.58	07 55.4	Im	0.9	2.0	16.0	14.5	66 ± 13
1987	12 41.44	13 24.0	SBc	6.2	1.9	11.1	7.6	304 ± 4
1992	12 41.65	12 23.4	Im	1.4	1.6	15.5	14.2	116 ± 6
2007	12 42.26	08 22.9	Im/BCD	0.6	1.9	15.2	13.5	74 ± 13
2023	12 43.02	13 36.4	SBc	2.5	2.0	13.9	11.4	176 ± 5
2034	12 43.61	10 26.2	Im	1.1	1.5	15.8	13.1	64 ± 13
2037	12 43.73	10 28.8	Im/BCD	1.8	2.3	15.8	13.1	50 ± 8
2070	12 45.86	08 45.6	Sa	4.5	2.0	11.5	7.4	417 ± 4

In order to understand the effective B-band limiting magnitude of the sample, we derived both the differential and the integral B-band luminosity functions (expressed, respectively,

in terms of $N(B_T^0)$ and $N(< B_T^0)$ vs. B_T^0 , i.e. the face-on apparent total magnitude) (Figs. 2a,b). From the comparison with the Virgo cluster luminosity function of Binggeli et al. (1988),

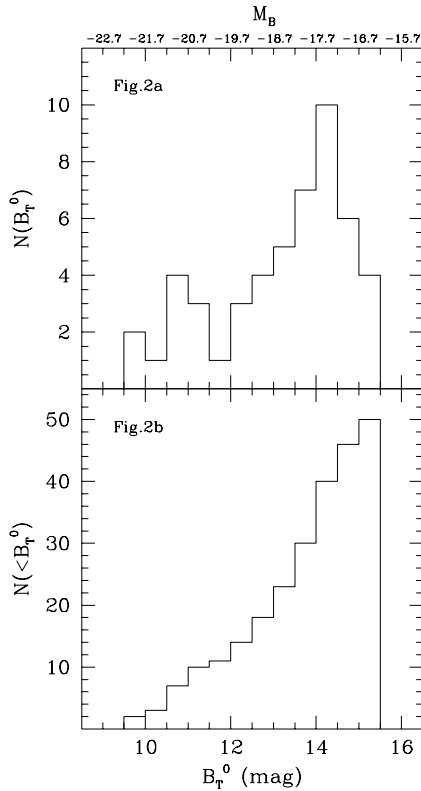


Fig. 2a and b. The differential **a** and the integral **b** B-band luminosity functions (expressed, respectively, in terms of $N(B_T^0)$ and $N(< B_T^0)$) vs. B_T^0 , i.e., the face-on apparent total magnitude). Absolute magnitudes are derived adopting a distance of 11 Mpc.

Table 2. Statistics of the TF residuals

Eq. No.	ave	adev	sdev	var	skew	curt
(1)	0.193	0.661	0.857	0.735	0.588	0.013
(2)	-0.192	0.760	1.006	1.013	-0.170	-0.229

we estimate a limiting magnitude of 14.5 B-mag for the completeness of our sample. As a consequence, 20% of the sampled galaxies are affected by incompleteness at the fainter B-magnitudes. However, Fig. 3 shows that there is no bias in the distribution of the “complete” and total subsamples of galaxies with respect to the NIR TF relation previously derived.

Moreover, we have assumed that the cluster depth effect (see Sect. 3 and Fig. 1a) is of the second order in the determination of the slope of the TF relation, while several authors have recently confirmed the large depth of Virgo (Schoeniger & Sofue 1997; Yasuda et al. 1997; Gavazzi et al. 1998). Galaxies located at different physical distances from the center of the cluster experience different astrophysical mechanisms which could affect several of their properties. We do not find any trends of the residuals of the present TF relation with the angular distance from the center of the cluster. However, Figs. 4a,b show that the TF residuals present an apparent mild correlation with the HI-deficiency of the galaxies (see Haynes & Giovanelli 1984; Haynes et al. 1985). The latter has been derived as in Guiderdoni & Rocca-

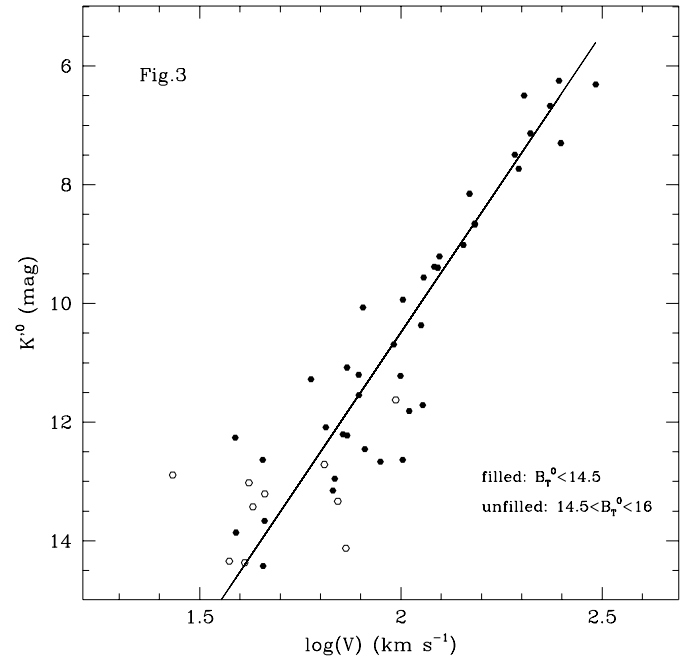


Fig. 3. The K' -band Tully-Fisher relation as in Fig. 1a. Here filled/empty hexagons represent galaxies of the “complete”/“un-complete” subsample (see text).

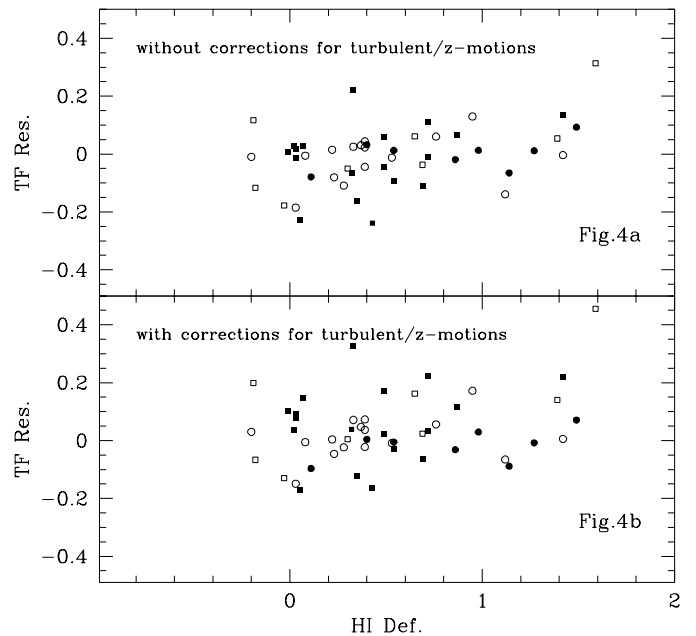


Fig. 4. Panels **a, b**: residuals of the fits of the TF relation in Figs. 1a,b vs. the HI-deficiency parameter (see text). Different symbols denote different morphological types as in Fig. 1a.

Volmerange (1985), in a distance-independent way, from the HI flux quoted in the previous sources of the HI linewidths, and is positively correlated with the angular distance from the center of the cluster (see Fig. 5). The trend shown in Figs. 4a,b is not due to a systematic underestimate of the maximum velocity in the HI-deficient galaxies (mainly early-type spirals), as discussed

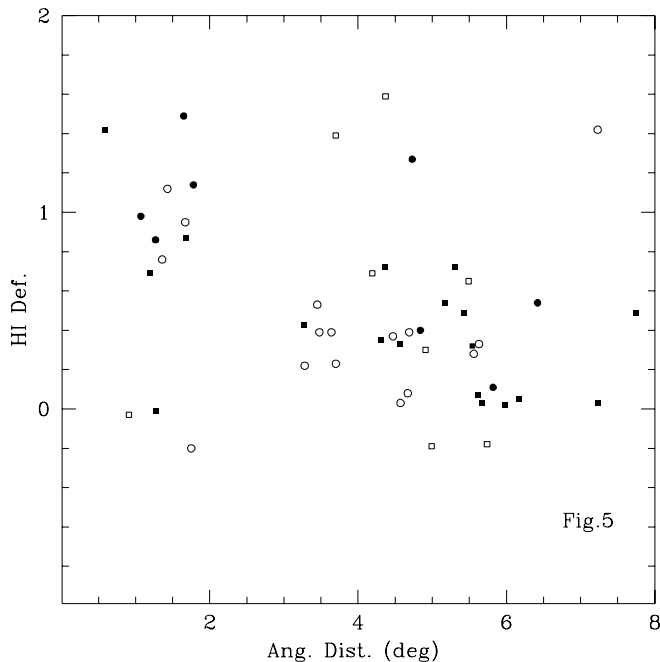


Fig. 5. The relation between the HI-deficiency parameter and the angular distance from the center of the cluster of the galaxies of the present sample. Different symbols denote different morphological types as in Fig. 1a.

in Sect. 2. We attribute it to the depth effect, even though a well-known anti-correlation of the HI-deficiency with lateness exists in the Virgo cluster (not shown). Distances for 34/50 of the sampled galaxies are available from Yasuda et al. (1997). They range between 8.98 and 36.32 Mpc, introducing an uncertainty of 0.91 mag in the Distance Modulus, in agreement with the value adopted in Fig. 1a (from Gavazzi et al. 1998). When the K' absolute magnitudes are derived for the 34 galaxies in common with Yasuda et al., the ensuing TF slope is -9.66 ± 0.30 (see Fig. 6), which is consistent with our previous determination (Eq. 2a). Therefore, we state that the cluster depth effect biases neither the linearity nor the slope of the present determination of the TF relation.

Fig. 6 also shows that the *observational* scatter is highly reduced and constant along the whole domain of velocities. However, we note that most of the low-velocity galaxies do not belong to Yasuda et al.'s sample. Therefore, we can only state that the increasing *observational* scatter with decreasing rotational velocity (Figs. 1a,b) is not inconsistent with claims that the *intrinsic* dispersion increases at lower luminosities (e.g. Giovanelli et al. 1997). Moreover, we note that the fairly deep sampling of the galaxy luminosity function gives some protection against a “Teerikorpi Cluster Population Incompleteness Bias” (CPIB) (Teerikorpi 1990; Sandage et al. 1995 and references therein; Giovanelli et al. 1997), affecting the present flux-limited sample of cluster galaxies. (We refer the reader to Sandage et al. 1995 and Teerikorpi 1997 for discussion of the CPI bias.) According to Sandage et al. (1995), the estimated completeness limit of 14.5 B-mag enables us to recover 90% of

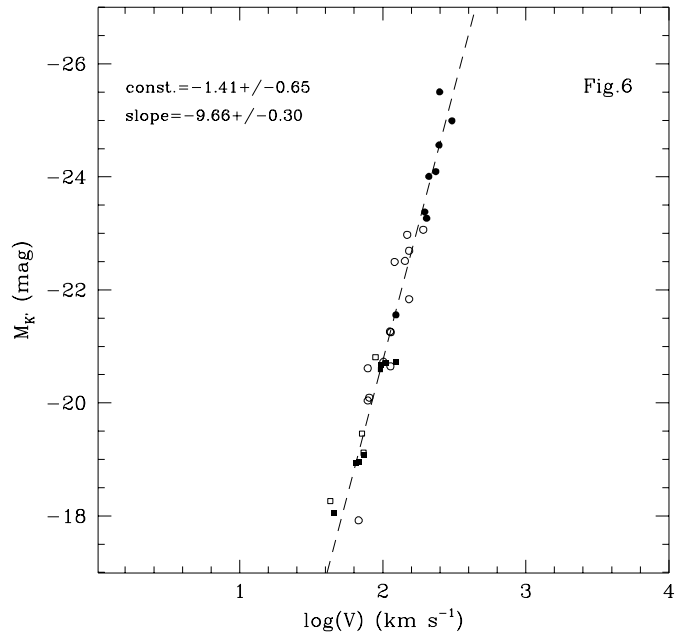


Fig. 6. The K' -band Tully-Fisher relation, where absolute magnitudes are plotted for the subsample of 34 galaxies with distances measured by Yasuda et al. (1998). Different symbols denote different morphological types as in Fig. 1a.

the *intrinsic* dispersion, hidden within the *observational* scatter. This result still holds not only for a Gaussian B-band luminosity function with an intrinsic dispersion of 0.6 mag (Sandage et al. 1995), which is not applicable for dwarf galaxies (cf. Binggeli et al. 1988), but also when arbitrary luminosity functions are considered (Tammann & Sandage 1982).

5. On the origin of the TF relation

The existence of a tight relation between luminosity and velocity for disk galaxies spanning a large range of luminosities, Hubble types and dark-to-luminous mass ratios (see Persic et al. 1996 for the B-band) must be related to some scale-free astrophysical properties or mechanisms. The cosmological origin of the Tully-Fisher relation has been extensively discussed in the literature, thanks to recent improvements of simulations (Steinmetz & Navarro 1998 and references therein) and of semi-analytic models (Somerville & Primack 1998 and references therein). However, it is difficult to understand how initial conditions can anticipate the low scatter of the TF relation (Eisenstein & Loeb 1996) and, therefore, some regulation or feedback mechanisms have been proposed to take place. It has been shown theoretically that self-regulating star-formation is potentially a rather powerful astrophysical mechanism to reproduce the TF relations in various optical photometric bands (Silk 1997; Elizondo et al. 1998). Here we analyze the interplay between dynamics/structure of giant and dwarf late-type galaxies (derived from NIR photometric observations) and star-formation, which comes out as a consequence of the complex connection between the gravitational potential of the galaxy and the gas-supply for star-formation in the latter scenario.

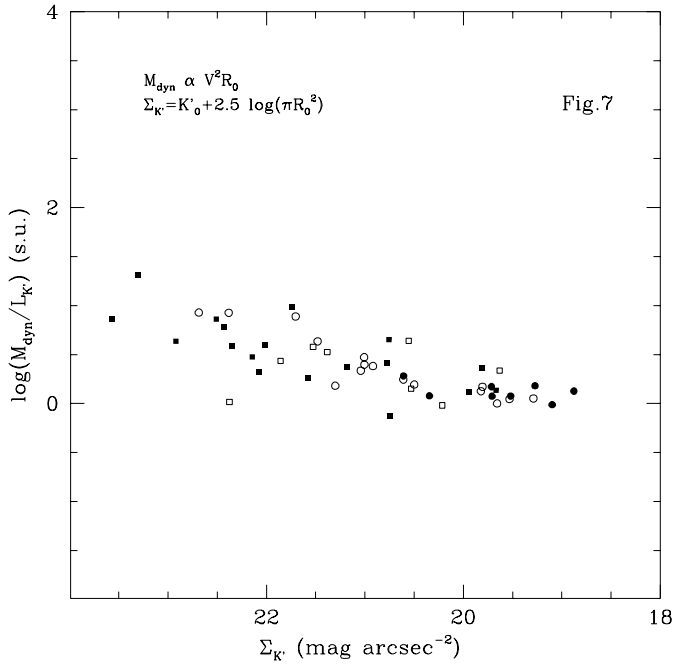


Fig. 7. The K' -band mass-to-light ratio vs. the average K' -band surface brightness. Different symbols denote different morphological types as in Fig. 1a.

5.1. Dynamical equilibrium

We have already illustrated the seminal ideas of Aaronson et al. (1979), who justified the existence of the TF relation mainly in terms of dynamical equilibrium. Such a “standard” scenario has already been disclaimed in the literature and is also not supported by the distribution of the present sample of galaxies in the NIR M/L - $\Sigma_{K'}$ plane (see Fig. 7). The values of the mass are derived from the rotational equilibrium law ($M \propto V_{Max}^2 R_0$), while the values of the average NIR surface brightness are given by $\Sigma_{K'} = K'_0 + 2.5 \times \log(\pi R_0^2)$ (where $R_0 = D_{25} / 2$ is corrected to the face-on value as in Giovanelli et al. 1995).

Fig. 7 shows a quite remarkable result, i.e. the existence of a smooth inverse correlation between M/L and Σ_0 .

This result is reminiscent of the behaviour of late-type galaxies within the B-band κ_2 - κ_3 plane of Burstein et al. (1997). The latter authors found that stellar systems (from globular clusters to galaxy clusters) distribute themselves in different planes inside a three-dimensional parameter system (called “ κ -space”), defined by galaxy mass, mass-to-light ratio and surface brightness. They also concluded that “the Tully-Fisher relation is the correct compromise projection to view the spiral-irregular planes nearly edge-on”.

Therefore, we have determined the K' -band Fundamental Plane (or κ -space) of the disk-components of the present sample of late-type galaxies (see also Pierini & Tuffs 1998). κ -dimensions are as in Burstein et al. (1997) (but in K' -band solar units, assuming K_\odot - $K'_\odot = 0$): disk scale-lengths (h) and central surface brightnesses (μ) are derived from the Marquardt-method (Press et al. 1992) fitting of an exponential law to the 60% outer region of the unidimensional surface brightness profiles (deter-

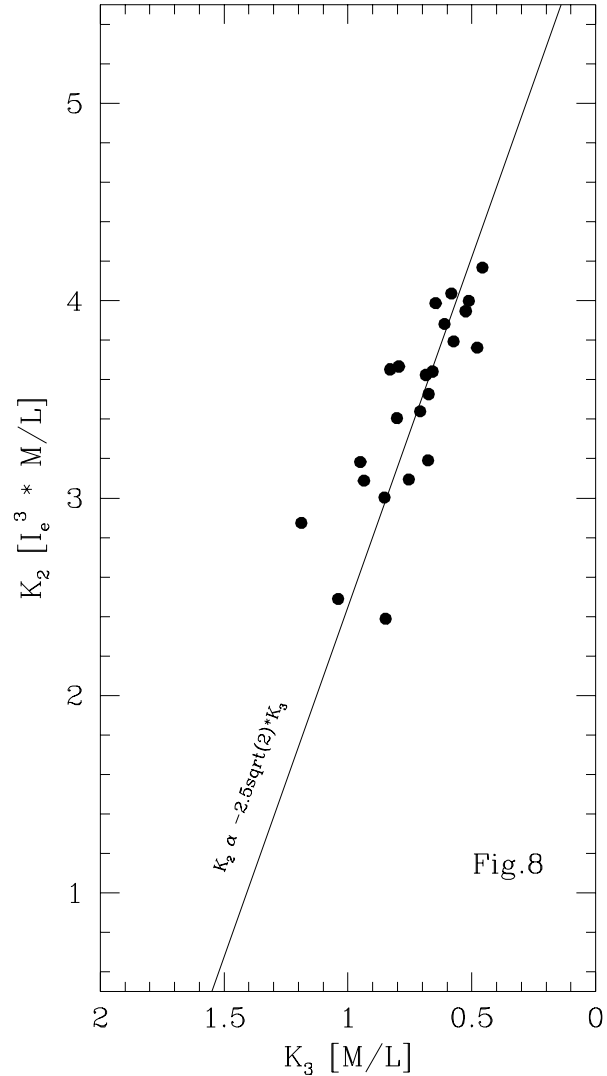


Fig. 8. The K' -band κ_2 - κ_3 plane of the disk-components of the subsample of 23 galaxies with best fits of the surface brightness distribution (see text). The straight line shows the slope expected if $L \propto V_{Max}^4$. Here galaxies are not differentiated in Hubble types.

mined as in Gavazzi et al. 1996b). They have been corrected for inclination according to the following recipes, statistically derived in Pierini (1997):

$$h_0 = h / (1 + 0.62 \log(a/b)),$$

$$\mu_0 = \mu + 2.5 \times 0.44 \log(a/b),$$

where a and b are, respectively, the major and minor axes. These two scaling parameters have been transformed into effective quantities as in Mao & Mo (1998). Moreover, HI linewidths have been lowered by 10% in bulge+disk systems to ideally remove the dynamical contribution of the bulge. Fig. 8 shows that the distribution of the 23 disks with best fits (reduced $\chi^2 \leq 2.5$) within the κ_2 - κ_3 plane is consistent with $\kappa_2 \propto -2.5\sqrt{2}\kappa_3$ (i.e.: $\log(M/L) \propto -3/(2.5\sqrt{2}+1)\log(I_e)$, where I_e is the effective intensity) for disk-systems, as expected if $L \propto V_{Max}^4$.

We believe that the κ -space is a powerful tool to analyze the dynamical, structural and stellar population properties of galaxies in a comprehensive way (but see Pahre et al. 1998), in relation also to their past history. Even though the physical origin of the κ -space is still not quite well understood, the validation of the NIR Tully-Fisher relation may hint at a physical connection between one of the astrophysical quantities determining the dynamical/structure properties (i.e., mass) and one of the astrophysical mechanism determining the mass-to-light ratio and the stellar surface brightness (i.e., star-formation). Such a conclusion is in agreement with the scenario of the self-regulating star-formation and is also consistent with previous analyzes of both the photometric properties (i.e., magnitudes, colours, gas content) and the structural properties (i.e., NIR-light concentration index, exponential disk scale-length and central surface brightness) of late-type galaxies (cf. Gavazzi et al. 1996a; Gavazzi & Scodreggio 1996; Pierini 1997).

5.2. Self-regulating star-formation

Seminal ideas of self-regulating star-formation as the physical origin of the TF relation are due to Silk (1997). His theoretical formulation of the B-band TF relation, from a simple scenario of galaxy formation, based mainly on supernova feedback and self-regulating star-formation rate in disks, is appealing, since it comes out without any assumptions on disk dynamics and cosmological evolution of structures. Within this framework, the steepening of the TF relation with increasing observing wavelength is directly explained when considering the contribution of the light of the progressively older stellar populations to the determination of the current star-formation rate ($\dot{\mu}_*$) (see Dopita & Ryder 1994). For example, adopting an observed slope of 2.1 for the B-band TF relation (in terms of luminosity vs. rotational velocity) and $\mu_B \sim \dot{\mu}_* \propto \mu_I^{0.64}$ (Dopita & Ryder 1994), Silk derives an I-band TF slope of 3.3, consistent with the value observationally found by Giovanelli et al. (1997). Recently, Elizondo et al. (1998) derived theoretical relations in agreement with the observed TF relations of giant galaxies in various photometric bands, using 3D hydrodynamical simulations of galaxy formation with supernova feedback and a multiphase medium. Moreover, they studied “the complex connection between depths of galaxy potential wells and the supply of gas for star formation” also in relation with different cosmological scenarios.

Here we try to gain an astrophysical settlement for the hint raised in the previous section, adopting the “extreme” scenario of Silk (1997) to predict the behaviour of the B and K' -band surface brightnesses of the present sample of galaxies. We assume a near-IR TF slope of 4 (in terms of luminosity vs. rotational velocity) and an I-band TF slope of 3.3. We note that non-linear optical TF relations have been claimed in the literature, when dwarf galaxies are considered (Matthews et al. 1998; Stil & Israel 1998). No observational results are given in the literature for the I-band. However, recent different theoretical models (Somerville & Primack 1998; Elizondo et al. 1998) produce optical TF relations which are linear over the

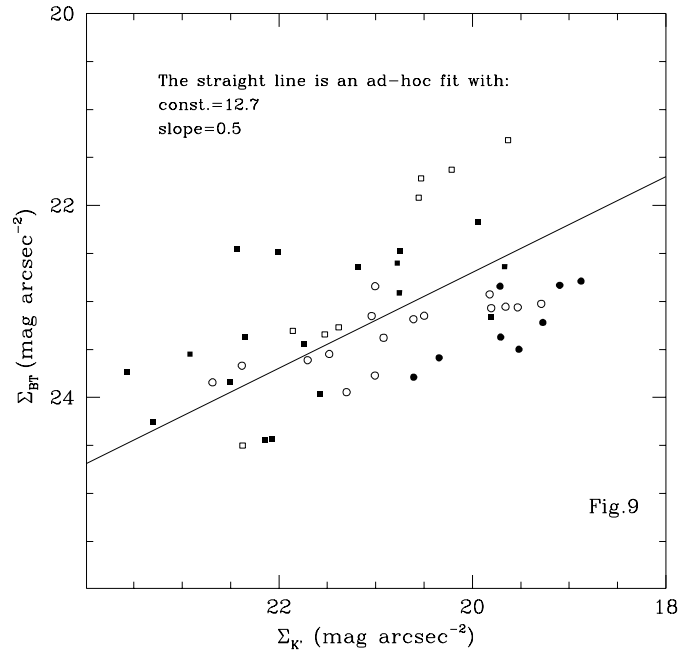


Fig. 9. Average B-band total surface brightness vs. the average K' -band surface brightness. Different symbols denote different morphological types as in Fig. 1a.

whole range of rotational velocities. We defer the analysis of such discrepancies to a future paper. From these two observational constraints, a Dopita & Ryder’s law of the type $\dot{\mu}_* \propto \mu_H^{0.5}$ is expected. The latter behaviour is confirmed by Fig. 9, where we adopt the average total (VCC) B-band surface brightness ($\Sigma_B = B_{T0} + 2.5 \times \log(\pi R_0^2)$) vs. the average K' -band surface brightness ($\Sigma_{K'}$).

However, we note that dwarf and giant galaxies seem to be systematically displaced in the y-axis by $\sim 2 \text{ mag arcsec}^{-2}$ (but the scatter in the plane is large). We suggest two major causes for such an effect. One is the existence of the optical/NIR colour-magnitude relation, which is mainly connected to the different star-formation histories of singular galaxies (e.g., Gavazzi et al. 1996a; Gavazzi & Scodreggio 1996). For the present sample of galaxies, the colour index $B_T - K'$ ranges within average values of 4 and 2, as lateness increases from Sa to BCD (Boselli et al. 1997). We stress that the present $B_T - K'$ include the contribution of the bulge (if present), and therefore bias the distribution of the giant bulge+disk systems toward redder colours. The other reason for the y-axis displacement is the potential over-estimate of the adopted correction for internal extinction (statistically derived in Gavazzi & Boselli 1996), due to the neglect of the metallicity-luminosity relation (see Skillman et al. 1989). As a consequence, this bias mainly affects the B-band magnitudes of dwarf galaxies.

6. Conclusions

We have selected a sample of 50 giant and dwarf late-type (Sa,...,Im-BCD; $B_T \leq 16$) member galaxies of the Virgo cluster, with available K' -band magnitudes and HI linewidths.

We find that, in the near-IR, the Tully-Fisher relation is linear within a range of 8 magnitudes, with $L \propto V_{\text{Max}}^4$. Therefore, even the faint, slow galaxies are rotationally supported systems, in agreement with van Zee et al. (1998). The present results complement previous work based on Virgo cluster giant late-type galaxies (i.e., Kraan-Korteweg et al. 1988; Peletier & Willner 1991) and extend the claim of Aaronson & Mould (1983) on the type-independence of the near-IR TF relation to Im-BCD galaxies. They contrast with recent determinations of the optical TF relation in dwarf galaxies (e.g., Matthews et al. 1998; Stil & Israel 1998). Such a discrepancy will be analyzed in a future paper. However, we note that overall linearity of the TF relation is a natural consequence of recent models of galaxy formation in various photometric bands (Somerville & Primack 1998; Elizondo et al. 1998).

It follows that the Tully-Fisher law must reflect some fundamental properties of disk-systems, which are not related to the morphological characteristics underlying the optical classification in Hubble types. This conclusion is strengthened by the distribution of the disks of the present sample of galaxies in the κ_2 - κ_3 plane. The relative tightness of such a distribution confirms the claim of Burstein et al. (1997) that the TF relation is the projection to view the multiple virial planes (or Fundamental Planes - FPs) for spiral and irregular galaxies close to edge-on.

The κ -space is a synthetic overview of the structural, dynamical and stellar population properties of stellar systems, and, therefore, it is also potentially expressing the complex connection between the gravitational potential of the galaxies and the supply of gas needed for star-formation. As a tentative proof, we show that the present sample of galaxies is distributed in the average B-band total surface brightness-average K'-band surface brightness plane according to expectations from the observed TF relations in various photometric bands and from the self-regulating star-formation scenario of Silk (1997).

Therefore, on the basis of the present data, we claim that the two building blocks for the physical basis of the Tully-Fisher relation, dynamical equilibrium and self-regulating star-formation, are connected.

Acknowledgements. We have benefitted greatly from the comments of the referee, P. Teerikorpi, which prompted us to a significant improvement of the paper. D.P. is also indebted to G. Gavazzi for useful discussions.

References

- Aaronson M., Huchra J., Mould J., 1979, ApJ 229, 1
 Aaronson M., Mould J., 1983, ApJ 265, 1
 Binggeli B., Sandage A., Tammann G.A., 1985, AJ 90, 1681
 Binggeli B., Sandage A., Tammann G.A., 1988, ARA&A 26, 543
 Binggeli B., Popescu C., Tammann G.A., 1993, A&AS 98, 275
 Boselli A., Tuffs R.J., Gavazzi G., Hippelein H., Pierini D., 1997, A&AS 121, 507
 Bottinelli L., Gouguenheim L., Paturel G., 1990, A&AS 82, 391
 Burstein D., Bender R., Faber S.M., Nolthenius R., 1997, AJ 114, 1365
 Cayatte V., van Gorkom J.H., Balkowski C., Kotanyi C., 1990, AJ 100, 604
 Condon J.J., Anderson M.L., Helou G., 1991, ApJ 376, 95
 Dalcanton J.J., Spergel D.N., Summers F.J., 1997, ApJ 482, 659
 De Blok W.J.G., McGaugh S.S., 1997, MNRAS 290, 533
 de Jong R.S., 1996, A&A 313, 45
 de Vaucouleurs G., de Vaucouleurs A., Corwin H.G., et al., 1991, Third Reference Catalogue of Bright Galaxies. Springer-Verlag, New York, Inc. (RC3)
 Dopita M.A., Ryder S.D., 1994, ApJ 430, 163
 Eisenstein D.J., Loeb A., 1996, ApJ 459, 432
 Elizondo D., Yepes G., Kates R., Müller V., Klypin A., 1998, astro-ph/9808287
 Gavazzi G., Boselli A., 1996, Astroph. Lett. Comm. 35, 1
 Gavazzi G., Scodreggio M., 1996, A&A 312, L29
 Gavazzi G., Pierini D., Boselli A., 1996a, A&A 312, 397
 Gavazzi G., Pierini D., Boselli A., Tuffs R., 1996b, A&AS 120, 489
 Gavazzi G., Boselli A., Scodreggio M., Pierini D., Belsole E., 1998, MNRAS, in press
 Giovanelli R., Haynes M.P., Salzer J.J., et al., 1995, AJ 110, 1059
 Giovanelli R., Haynes M.P., Herter T., et al., 1997, AJ 113, 53
 Guiderdoni B., Rocca-Volmerange B., 1985, A&A 151, 108
 Haynes M.P., Giovanelli R., 1984, AJ 89, 758
 Haynes M.P., Giovanelli R., Chincarini G., 1985, ARA&A 22, 445
 Hoffman G.L., Helou G., Salpeter E.E., Glosson J., Sandage A., 1987, ApJS 63, 247
 Huchtmeier W.K., Richter O.G., 1989, A&A 210, 1
 Kraan-Korteweg R.C., Cameron L.M., Tammann G.A., 1988, ApJ 331, 620
 Mao S., Mo H.J., 1998, MNRAS 297, L71
 Matthews L.D., van Driel W., Gallagher J.S., 1998, AJ 116, 2196
 Mo H.J., Mao S., White S.D.M., 1998, MNRAS 295, 319
 McGaugh S.S., Bothun G.D., 1994, AJ 107, 530
 Pahre M.A., Djorgovski S.G., de Carvalho R.R., 1998, AJ 116, 1591
 Peletier R.F., Willner S.P., 1991, ApJ 382, 382
 Peletier R.F., Willner S.P., 1993, ApJ 418, 626
 Persic M., Salucci P., Stel F., 1996, MNRAS 281, 27
 Pierce M.J., Tully R.B., 1988, ApJ 330, 579
 Pierini D., 1997, Ph.D. thesis, University of Milano
 Pierini D., Tuffs R., 1998, In: Richtler T., Braun J.M. (eds.) Proceedings of the Bonn/Bochum Graduiertenkolleg Workshop: The Magellanic Clouds and Other Dwarf Galaxies. Physikzentrum Bad Honnef. Shaker Verlag, Aachen, ISBN 3-8265-4457-9, p. 281
 Press W., Teukolsky S., Vetterling W., Flannery B., 1992, Numerical Recipes in Fortran. II Edition, C.U.P., p. 678
 Sandage A., Tammann G., Federspiel M., 1995, ApJ 452, 1
 Schoeniger F., Sofue Y., 1997, A&A 323, 14
 Silk J., 1997, ApJ 481, 703
 Skillman E.D., Kennicutt R.C., Hodge P.W., 1989, ApJ 347, 875
 Somerville R.S., Primack J.R., 1998, astro-ph/9802268
 Steinmetz M., Navarro J.F., 1998, astro-ph/9810151
 Stil J.M., Israel F.P., 1998, astro-ph/9810151
 Tammann G., Sandage A., 1982, In: West R.M. (ed.) Highlights Astronomy, Vol.6, Reidel, Dordrecht, p. 301
 Teerikorpi P., 1990, A&A 234, 1
 Teerikorpi P., 1997, ARA&A 35, 101
 Tully R.B., Fisher J.R., 1977, A&A 54, 661
 Tutui Y., Sofue Y., 1997, A&A 326, 915
 van Zee L., Skillman E.D., Salzer J.J., 1998, AJ 116, 1186
 Yasuda N., Fukugita M., Okamura S., 1997, ApJS 108, 417
 Zwaan M.A., van der Hulst J.M., de Blok W.J.G., McGaugh S.S., 1995, MNRAS 273, L35